

Self-Pulsation Dynamics in GaAs/AlGaAs Quantum Cascade Lasers*

Liu Junqi, Liu Fengqi†, Li Lu, Shao Ye, Guo Yu, and Wang Zhanguo

(Key Laboratory of Semiconductor Materials Science, Institute of Semiconductors,
Chinese Academy of Sciences, Beijing 100083, China)

Abstract: Quasi-continuous wave lasing spectra of GaAs/AlGaAs quantum cascade lasers emitting at $9.76\mu\text{m}$ are characterized by step-scan time-resolved Fourier transform infrared spectroscopy. Pronounced self-pulsation in stacked emission spectra is observed in the driving current duration. Self-heating accumulation in the active region affects the electron relaxation and transport greatly. Thermally-induced carrier occupation of the higher sublevels in an injector can leak out through a resonant condition with the continuum states above the next injector, which will be facilitated by the fourth sublevel of the coupled quantum wells active region. The leaking process arising from the periodic breaking and recovering of resonant tunneling accounts for the physical mechanism of the self-pulsed effect in stacked emission spectra.

Key words: quantum cascade laser; self-pulsation; molecular beam epitaxy

PACC: 6855; 4255P **EEACC:** 4320J; 2520D

CLC number: TN365 **Document code:** A **Article ID:** 0253-4177(2007)S0-0044-04

1 Introduction

The performance of mid-infrared GaAs/ $\text{Al}_x\text{Ga}_{1-x}\text{As}$ quantum cascade lasers (QCLs) has been improved remarkably since their inception. However, the main difficulty on the route to high power and continuous-wave operation at room temperature is still the rather large threshold current density of these devices. Therefore, much effort has been invested into understanding the underlying physical mechanism affecting the lasing process. The Al mole fraction is a central parameter influencing not only the lasing wavelength, but also the temperature performance of QCLs. The temperature limitation of the original GaAs/ $\text{Al}_{0.33}\text{Ga}_{0.67}\text{As}$ QCLs was ascribed to the inefficient carrier injection from the injector into the upper laser level, which results from the thermally induced leakage current into continuum states^[1,2]. Increasing the carrier confinement within the heterostructure will strongly improve the thermal behavior of these devices. A larger conduction band offset for GaAs/ $\text{Al}_{0.45}\text{Ga}_{0.55}\text{As}$ structure is expected

to optimize the injection efficiency and improve the population ratio of upper and lower laser levels^[3~5]. Injector doping density is another crucial parameter for the lasing performance. The dependence of the threshold current density on the doping density has been theoretically and experimentally investigated^[6~8], and the optimum value has been determined to be about $(6\sim 7) \times 10^{11}\text{cm}^{-2}$. Although these results speed up the research of this kind of novel devices, the underlying reason for the lower average power of GaAs/AlGaAs QCLs compared to InP-based lasers in a larger drive pulse is not clear. In this paper, we concentrate on disclosing this problem by the investigation of the lasing spectra driven by a relatively large current pulse (on the order of a microsecond) above liquid nitrogen temperature.

2 Processing and measurement

The QCL structure, grown by molecular beam epitaxy (MBE) on an n^+ ($n = 2 \times 10^{18}\text{cm}^{-3}$) GaAs substrate, consists of upper and lower n^+ ($n = 6 \times 10^{18}\text{cm}^{-3}$, $1\mu\text{m}$ thick) GaAs cladding layers, and low doped ($n = 4 \times 10^{16}\text{cm}^{-3}$, $3.75\mu\text{m}$ thick) spac-

* Project supported by the National Science Fund for Distinguished Young Scholars (No. 60525406), the Key Program of the National Natural Science Foundation of China (No. 60136010), the State Key Development Program for Basic Research of China (No. G20000683-2), and the National High Technology Research and Development Program of China (Nos. 2001AA311140, 2005AA31G040)

† Corresponding author. Email: fqliu@red.semi.ac.cn

Received 16 November 2006

er layers surrounding the core region, which contains 40 repetitions of active regions/injector regions, as published by Page *et al.* [3]. The sequence of one period starting from the injector is **4.6**, **1.9**, **1.1**, **5.4**, **1.1**, **4.8**, **2.8**, **3.4**, **1.7**, **3.0**, **1.8**, **2.8**, **2.0**, **3.0**, **2.6**, and **3.0**nm (where bold script denotes $\text{Al}_{0.45}\text{Ga}_{0.55}\text{As}$ and normal script GaAs). Two periods of the superlattice injector (underlined layers) were doped to an optimum density of $(6\sim 7) \times 10^{17} \text{ cm}^{-3}$ in order to achieve a significant gain and, at the same time, avoid a considerable increase in the threshold current [8].

After MBE growth, the wafer was processed into $45\mu\text{m}$ -wide double-channel ridge devices by reactive ion etching to a depth penetrating through the waveguide core. A 300nm -thick SiO_2 layer was then grown by chemical vapor deposition for insulation around the ridges. After opening a $25\mu\text{m}$ -wide window through the insulation layer for current injection on each of the ridges, a non-alloyed Ti/Au Ohmic contact was deposited to the top layer. Then the wafer was thinned to about $120\mu\text{m}$, and an alloyed AuGeNi/Au contact was deposited on the backside. The devices were cleaved into laser bars, leaving both facets uncoated and a soldered epilayer down to copper holders with indium, then wire bonded.

The lasers were mounted on a temperature-controlled cold finger in a vacuum liquid nitrogen cryostat. The spectral measurements were carried out with a BRUKER EQUINOX 55 Fourier transform infrared (FTIR) spectrometer in the step-scan time-resolved mode, and a normal resolution of 2cm^{-1} was applied.

3 Results and discussion

Figure 1 shows the typical three-dimensional spectrum stacked in the time domain with the laser driven by a pulse of 1kHz and 1% duty cycle at 80K . The sampling principle of the spectra is presented in Ref. [9]. Shown in Fig. 2 is the relation between lasing intensity at laser frequency and the pulse duration. In this experiment a time resolution of 50ns was used, and the intensity of emission is normalized in all figures. Obviously, the laser emission becomes unstable and pulsed in the current duration. This self-pulsation during the lasing process may degrade the average power noticeably. The fluctuation of lasing intensity can be

ascribed to the temporal change of the population inversion of the upper and lower laser levels (subbands). What makes this change? As we know, at higher injector doping density the electrons behave a thermalized distribution in all the remaining subbands [10]. Driven with a rather large current pulse, thermal accumulation in the central part of the device cannot be evacuated effectively. This thermal effect enhances the thermally activated electron leakage in the injector and the upper laser sublevel in the active region. The reduction of the injection efficiency into the upper laser sublevel will deteriorate the lasing performance established by the equilibrium condition.

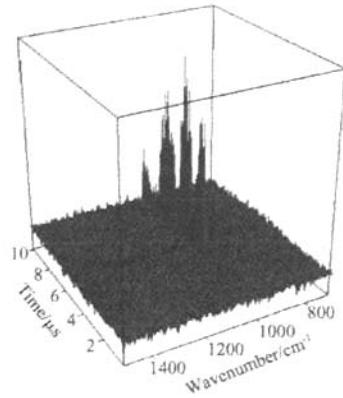


Fig. 1 Stacked emission spectrum of a 2mm -long and $45\mu\text{m}$ -wide laser obtained from the step-scan time-resolved FTIR with time resolution of 50ns . The temperature of the heat sink was held at 80K during the measurement.

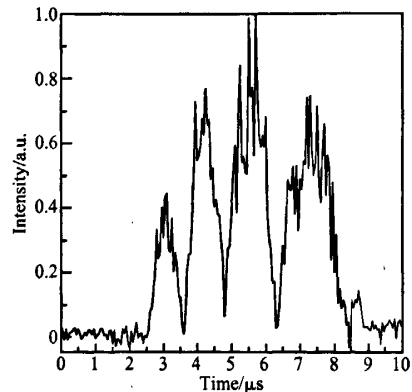


Fig. 2 Emission intensity at the lasing frequency (1024.4cm^{-1} , i. e. $9.76\mu\text{m}$) versus the drive pulse duration, extracted from the three-dimensional spectrum in Fig. 1

In order to determine the influence of the waveguide core design on the lasing performance, conduction band structure calculations were carried out based on the one-dimensional Schrodinger equation for an external electric field strength $F = 53\text{kV/cm}$. Figure 3 shows that there is a sublevel E_4 with 65meV above the laser uplevel E_3 that establishes a bridge between the injector miniband and the collector continuum states. The transmission of the injector was calculated at $F = 53\text{kV/cm}$ and is shown in Fig. 4. The sublevel E_4 shows a larger transmission coefficient than others including the lowest one, E_1 , in the active region. Therefore, E_4 in the active region may act as a leakage channel when the device is lasing and the upper sublevels in the injector are being filled with thermalized electrons.

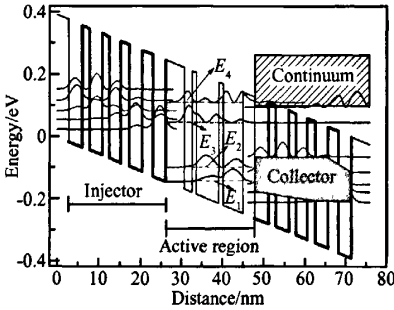


Fig. 3 Calculated conduction band diagram of the GaAs/Al_{0.45}Ga_{0.55}As QCL for $F = 53\text{kV/cm}$. E_1, E_2, E_3 and E_4 denote the laser sublevels.

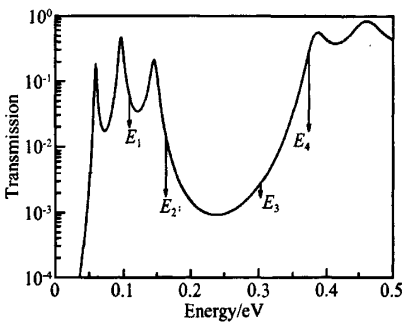


Fig. 4 Calculated transmission coefficient of the collector shown in Fig. 3 for $F = 53\text{kV/cm}$. E_1, E_2, E_3 and E_4 are in accordance with what appears in Fig. 3.

We introduce the linear rate equations^[5,11] to explain the self-pulsed effect. For the three-level system of the active region, we assume that the population of E_3 is n_3 , of E_2 is n_2 , the relaxation time from E_3 to E_2 is τ_{32} , escaping from E_3 to oth-

er states is τ_{esc} , the extraction from E_2 is τ_{ext} , and the maximum carrier injection into E_3 is I_0 .

$$\frac{dn_3}{dt} = I_0 - \frac{n_3}{\tau_{32}} - \frac{n_3}{\tau_{esc}} \quad (1)$$

$$\frac{dn_2}{dt} = \frac{n_3}{\tau_{32}} - \frac{n_2}{\tau_{ext}} \quad (2)$$

According to τ_{32} , τ_{esc} , and τ_{ext} are of subpicosecond order, and steady-state conditions can be assumed in a relatively short time segment. Thus, we can obtain the following equations by Eq. (1):

$$I_0 = n_3 \left(\frac{1}{\tau_{32}} + \frac{1}{\tau_{esc}} \right) = \frac{n_3}{\tau_3} \quad (3)$$

and by Eq. (2):

$$\frac{n_3}{n_2} = \frac{\tau_{32}}{\tau_{ext}} = \rho_p \quad (4)$$

According to Eqs. (3) and (4), the population inversion is

$$\Delta n = n_3 - n_2 = \left(1 - \frac{1}{\rho_p} \right) n_3 = \frac{\rho_p - 1}{\rho_p} I_0 \tau_3 \quad (5)$$

For a longer drive pulse compared to the steady-state cycles, the population inversion will fluctuate due to the degradation of carrier injection into E_3 . In this situation, we introduce a correctional factor $I(t)$ to the carrier injection I_0 . The temporal population inversion changes into

$$\Delta n(t) = \frac{\rho_p - 1}{\rho_p} I(t) I_0 \tau_3 \quad (6)$$

The factor $I(t)$ is affected by the hot-carrier dynamics. There is a competitive relation between intercarrier thermalization and phonon-assisted relaxation in QCLs^[10]. When the hot electrons in the injector relax their large amount of energy supplied by the applied bias mainly via carrier-carrier scattering, there are two consequences: one is the large coupling constant between electron temperature and lattice temperature, which results in a large temperature difference between them^[12,13]; and the other is the thermal distribution of electrons in all the injector sublevels. The occupation of hot electrons in the high sublevels of the injector enhances the carrier leakage through the E_4 resonated with the continuum levels. As a result, the population inversion deteriorates. At the same time, the large temperature difference between electrons and lattice boosts the carrier relaxation through phonon-assistance. This carrier-cooling process increases the carrier injection into E_3 and improves the population inversion. The incessant competition between carrier-carrier and phonon-carrier relaxation during the pulse duration makes

a wave-like correctional factor $I(t)$. This is consistent with our results obtained by the time-resolved spectra. The envelope of these pulsed lasing lines may be rooted in the thermal fluctuation of device mounting.

4 Conclusion

In summary, we have investigated the lasing performance of GaAs/Al_{0.45}Ga_{0.55}As QCLs at a relatively large drive pulse. The emission intensity in large pulse duration takes pronounced self-pulsation. The carrier dynamics in the injector remarkably affects the population inversion of the upper and lower laser level. The competition between different relaxation modes results in the fluctuation of population inversion. The existence of the fourth sublevel in the active region facilitates the carrier leakage in the injector through a resonance with the continuum states above the next injector. The self-pulsed effect in the lasing process accounts for most of the degradation of the average optical power at a rather large drive pulse.

Acknowledgments The author would like to acknowledge the help of P. Jin, P. Liang, Y. Hu, and H. Sun.

References

- [1] Sirtori C, Kruck P, Barbieri S, et al. GaAs/Al_xGa_{1-x}As quantum cascade lasers. *Appl Phys Lett*, 1998, 73:3486
- [2] Indjin D, Harrison P, Kelsall R W, et al. Influence of leakage current on temperature performance of GaAs/AlGaAs quantum cascade lasers. *Appl Phys Lett*, 2002, 81:400
- [3] Page H, Becker C, Robertson A, et al. 300K operation of GaAs-based quantum-cascade laser at $\lambda \approx 9\mu\text{m}$. *Appl Phys Lett*, 2001, 78:3529
- [4] Ortiz V, Becker C, Page H, et al. Thermal behavior of GaAs/AlGaAs quantum-cascade lasers: effect of the Al content in the barrier layers. *J Cryst Growth*, 2003, 251:701
- [5] Schrottke L, Lu S L, Hey R, et al. Population inversion and threshold current densities: a comparison of GaAs/(Al,Ga)As quantum-cascade structures with different barrier heights. *J Appl Phys*, 2005, 97:123104
- [6] Giehler M, Hey R, Kostial H, et al. Lasing properties of GaAs/(Al,Ga)As quantum-cascade lasers as a function of injector doping density. *Appl Phys Lett*, 200, 82:671
- [7] Giehler M, Kostial H, Hey R, et al. Effect of free-carrier absorption on the threshold current density of GaAs/Al(Ga)As quantum-cascade lasers. *J Appl Phys*, 2004, 96:4755
- [8] Jovanović V D, Indjin D, Vukmirović N, et al. Mechanisms of dynamic range limitations in GaAs/AlGaAs quantum-cascade lasers: influence of injector doping. *Appl Phys Lett*, 2005, 86:21117-1
- [9] Liu J Q, Lu X Z, Guo Y, et al. Application of step-scan FTIR to the research of quantum cascade lasers. *Chin Opt Lett*, 2005, 3:603
- [10] Iotti R C, Rossi F. Carrier thermalization versus phonon-assisted relaxation in quantum-cascade lasers: a Monte Carlo approach. *Appl Phys Lett*, 2001, 78:2902
- [11] Donovan K, Harrison P, Kelsall R W. Self-consistent solutions to the intersubband rate equations in quantum cascade lasers: analysis of a GaAs/Al_xGa_{1-x}As device. *J Appl Phys*, 2001, 89:3084
- [12] Harrison P, Indjin D, Kelsall R W. Electron temperature and mechanisms of hot carrier generation in quantum cascade lasers. *J Appl Phys*, 2002, 92:6921
- [13] Spagnolo V, Scamarcio G, Schrenk W, et al. Influence of the band-offset on the electronic temperature of GaAs/Al(Ga)As superlattice quantum cascade lasers. *Semicond Sci Technol*, 2004, 19:S110

GaAs/AlGaAs 量子级联激光器自脉动动力学*

刘俊岐 刘峰奇[†] 李路 邵焯 郭瑜 王占国

(中国科学院半导体研究所 半导体材料科学重点实验室, 北京 100083)

摘要: 利用步进扫描时间分辨傅里叶变换红外光谱,研究了波长 $9.76\mu\text{m}$ GaAs/AlGaAs 量子级联激光器的准连续波激射谱. 在驱动电流周期内, 时间上堆叠的发射谱能够观察到明显的光强自脉动现象. 有源区中的自加热积累大大影响了电子的驰豫和输运性质. 热引起的在注入区较高子能级中占据的载流子由于这些子能级与下一注入区的连续态形成共振条件而泄露, 而耦合阱有源区中第四子能级的存在加快了这个过程. 周期性破坏和恢复的共振条件所引起的载流子泄露在很大程度上导致了时域堆叠光谱的自脉动.

关键词: 量子级联激光器; 自脉动; 分子束外延

PACC: 6855, 4255P **EEACC:** 4320J, 2520D

中图分类号: TN365

文献标识码: A

文章编号: 0253-4177(2007)05-0044-04

* 国家杰出青年科学基金(批准号:60525406), 国家自然科学基金重点项目(批准号:60136010), 国家重点基础研究发展规划(批准号:G20000683-2)及国家高技术研究发展计划(批准号:2001AA311140 和 2005AA31G040)资助项目

[†] 通信作者. Email: fqliu@red.semi.ac.cn

2006-11-16 收到